

## Online optical verification system for sheet-metal processing

Takamasa Suzuki\*<sup>a</sup>, Kotaro Sato<sup>a</sup>, Shogo Muramatsu<sup>b</sup>, Mitsuyoshi Murata<sup>c</sup>, and Toshiro Oitate<sup>d</sup>

<sup>a</sup> Niigata Univ., Graduate School of Science and Tech., 8050 Ikarashi 2, Niigata, 950-2181 Japan

<sup>b</sup> Niigata University, Faculty of Engineering, 8050 Ikarashi 2, Niigata, 950-2181 Japan

<sup>c</sup> TechnoCare Corp., 1-25-8 Sobudai, Sagamihara, Kanagawa, 228-0824 Japan

<sup>d</sup> Totsuka Metal Industry CO., LTD., 1102-1 Koseki, Tsubame, Niigata, 959-1286 Japan

### ABSTRACT

We propose and demonstrate a novel processing cycle for sheet-metal working based on the computerized image processing techniques. The interconnected test system based on the cross network communication enables the effective fabrication cycle that realizes automatic inspection, quick delivery, and cost reduction.

**Keywords:** Sheet-metal processing, cross network, optical verification, image processing

### 1. INTRODUCTION

Sheet-metal working is one of the most important processes in manufacturing commercial products, such as small parts in automobile, electronic devices, and electric appliances, because these products require metal chassis. However, sheet-metal working has a small profit margin because it does not require advanced techniques and is difficult to differentiate one's output from one's business competitors. Many companies in sheet-metal processing seek a more effective way to manufacture their products. In sheet-metal processing, a series of fabrication steps, such as cutting, boring, and punching is implemented based on an initial drawing (Fig. 1). Since product failure happens due to mistakes in the mold insert, programming glitches in the numerical control (NC) machine, and typing errors in the Drawing Exchange Format (DXF) data, prototype inspection before mass production is very important. That is, a cost reduction in the fabricating process is the key to differentiation.

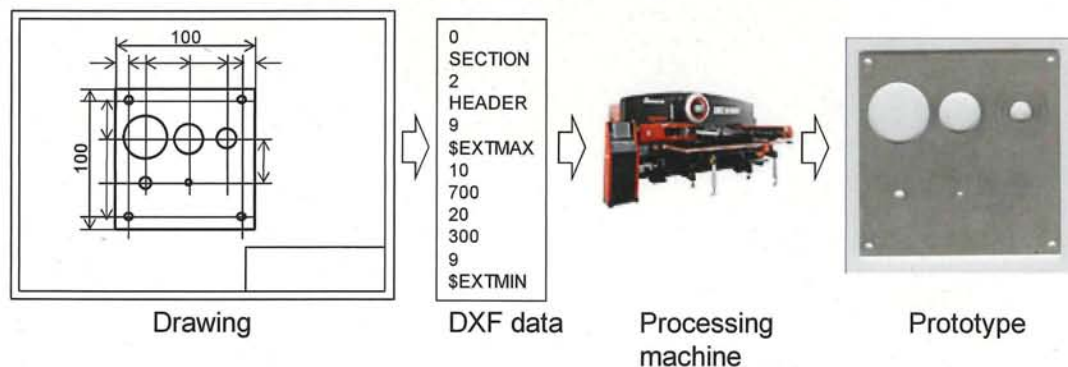


Fig. 1 Basic sheet-metal processing.

Figure 2 shows the conventional sheet-metal production cycle. The inspections of small and medium-sized works are still conducted manually by using conventional devices, such as a ruler, caliper, and micrometer. Because this kind of inspection takes a long time, it is an obstacle to quick delivery and cost reduction. In the case of a sheet metal product that has hundreds of holes of different shapes, an inspection takes more than half a day even for an expert. Moreover, since the inspection is implemented once before mass production begins, numerous defective products will be produced if some accidents such as misfeed or breakage of the mold occur during the manufacturing process. We have been unable to find economical and automatic inspection systems for sheet metal processing at present.

\*takamasa@eng.niigata-u.ac.jp; phone / fax 81 25 262-7215

In this paper, we describe a processing cycle that promotes greater efficiency and productivity. We also describe some experiments that demonstrate the optical testing systems, which is one of the most important parts in the proposed processing cycle.

The proposed sheet-metal production cycle shown in Fig. 3 applies computerized image processing techniques to the inspection. This enables automatic inspection, quick delivery, and cost reduction based on the cross network communication. Inspecting samples during mass production is easy, and it prevents massive product failures. The test data or related web contents can be shared between companies in the same trade so as to increase production efficiency.

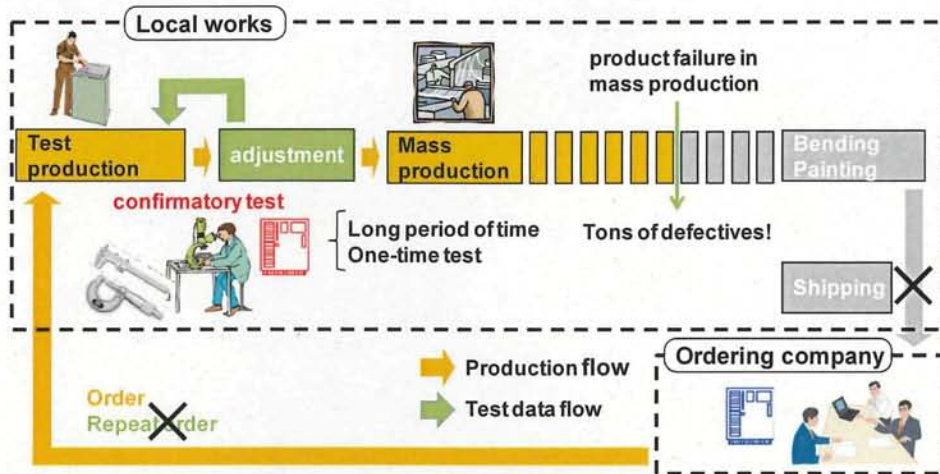


Fig. 2 Conventional sheet-metal production cycle.

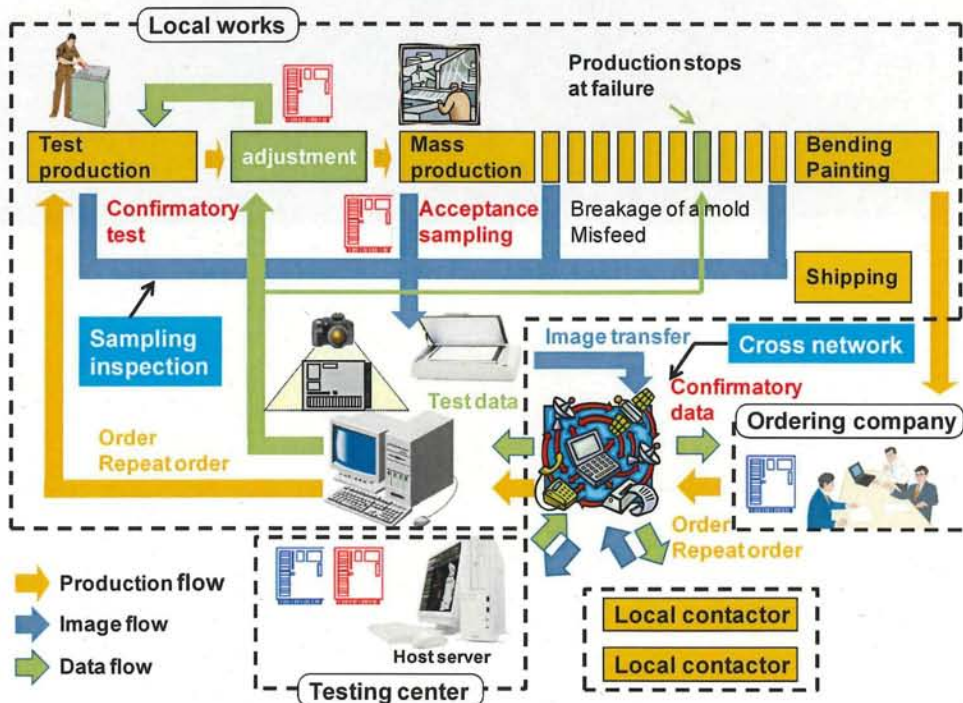


Fig. 3 Unified sheet-metal production cycle assisted by the cross network.

Moreover, as shown in Fig. 4, businesses and ordering companies can discuss the arrangements for manufacturing by reference to the same stored data. Thus quick orders or repeat orders from an ordering company are easily realized through the cross network communication.

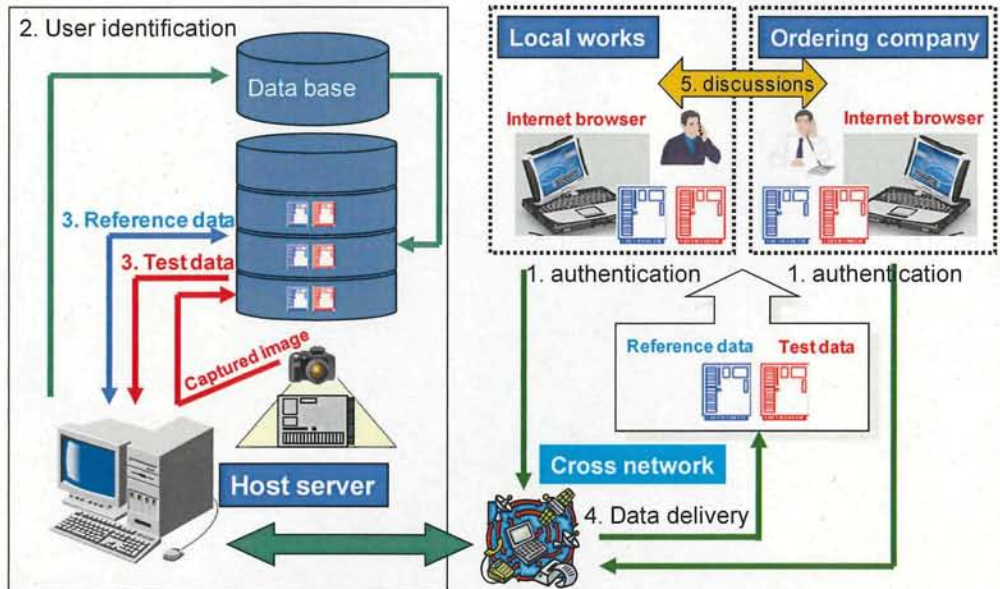


Fig. 4 An illustration of the discussion of the arrangements for manufacturing between local works and ordering company.

## 2. SPECIFICATIONS OF THE SYSTEM

The goal specifications of the testing system are shown in Table 1. A flat bed scanner and digital camera are used as the imaging devices. An applicable maximum size is the A1 paper size. When an economical A3 size scanner is used, the total testing time is 10 minutes at an accuracy of 0.5 mm. Because an A1 size scanner is not so common and very expensive, we put considerable effort into building a digital camera into the testing system. The specifications of the digital camera system outstrip that of the scanner system. The last row shows the resolution of the imaging devices used in the experiments. The resolution of the digital camera is 5616×3744 pixels. Table 2 indicates the specifications of the host server. It administrates user authentication, related web contents, relevant data, and security management on the network.

Table 1 Specifications of the testing system.

Imaging device	Flatbed scanner		Digital camera
Maximum size	A3	A1	A1
Image capture time (min)	3	6	10 (s)
Image processing time (min)	5	10	10
Verification time (min)	2	4	4
Total testing time (min)	10	20	14
Accuracy (mm)	0.5	1.0	0.5
Resolution	2400 dpi	6400 dpi	5616×3744 (21 Mpixels)

Table 2 Specifications of the host server.

User authentication	
WEB contents	User guide
	Information of participating company
Administration of the data	bidirectional communication of the CAD data
	Data base
Security management	

### 3. IMAGING DEVICES

#### 3.1 Flatbed scanner

We first examined the characteristics of the A3 size flatbed scanner as the imaging device (Fig. 5(a)). It possesses both reflective and transmissive modes for image acquisition at a resolution of 2400 dpi as shown in Figs. 5(b) and 5(c), respectively. There is a possibility that shadows will be observed at the position close to the edges of the holes. The shadows cast by the object (and the resulting shaded areas on the scanner) become large as the thickness of the object increases, as shown in Fig. 6.

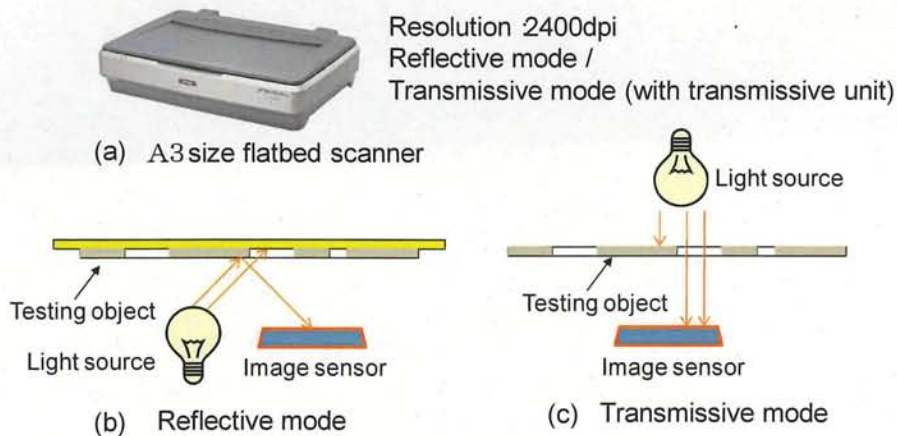


Fig. 5 Flatbed scanner as an imaging device.

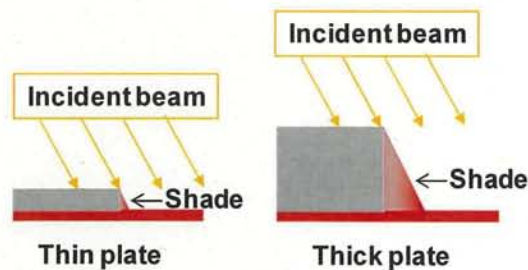


Fig. 6 An illustration of the shaded area dependence on the thickness of a target.

The captured images are shown in Figs. 7 and 8, respectively, in reflective mode and transmissive mode. The random patterns such as many kinds of scratches, the textures of the materials, and drawing lines painted by a pen on the surface of the object are all captured in the reflective mode as shown in Fig. 7(a). The magnified image of a part of Fig. 7(a) is shown in Fig. 7(b), showing some shadows and images of the wall surface at the edges of the holes. On the other hand, random patterns and shaded areas are not detected in the transmissive mode as shown in Fig. 8(a). Only the images of the wall surface are observed in the magnified image shown in Fig. 8(b).

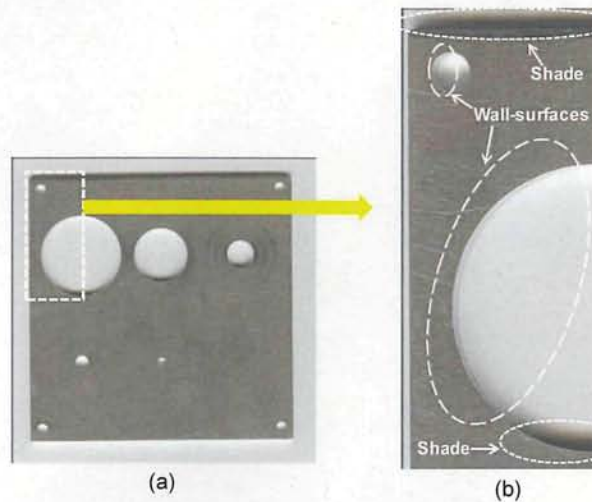


Fig. 7 Images of the sheet metal sample scanned by the flatbed scanner in reflective mode; (a) whole image and (b) magnified image.

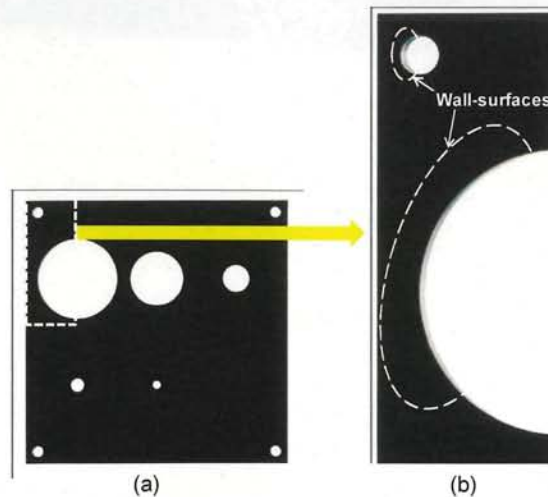


Fig. 8 Images of the sheet metal sample scanned by the flatbed scanner in transmissive mode; (a) whole image and (b) magnified image.

### 3.2 Digital camera

Recently, performance of digital cameras has been getting better and the price has been getting cheaper. As an imaging device, this is suitable for our purpose. Figure 9 shows a simple diagram of the setup of the image capture system utilizing a digital camera. This system works in the transmissive mode. The image capturing speed is very fast compared

with the flatbed scanner system because no mechanical scanning is required. The test object placed on the diffuser panel is irradiated by the light source and imaged onto the digital camera.

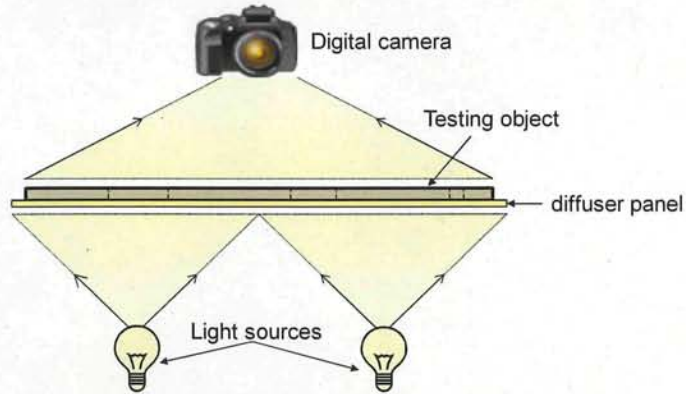


Fig. 9 Image capture system with a digital camera.

To confirm the resolution, we took the image of a test template (Fig. 10(a)) that has multiple slits of width 0.5 mm. The size of the plate was 400 mm×200 mm. After extracting a small segment from Fig. 10(a), we observed the width of the slit over a width of five pixels in Fig. 10(b). This satisfies the accuracy of 0.5 mm indicated in Table 1.

One of the major problems in a digital camera is the image distortion caused by a wide-angle lens. Although this kind of lens is useful when a compact setup is required, the normal image (Fig. 11(a)) is distorted with barrel distortion (Fig. 11(b)). This distortion should be corrected with image processing.

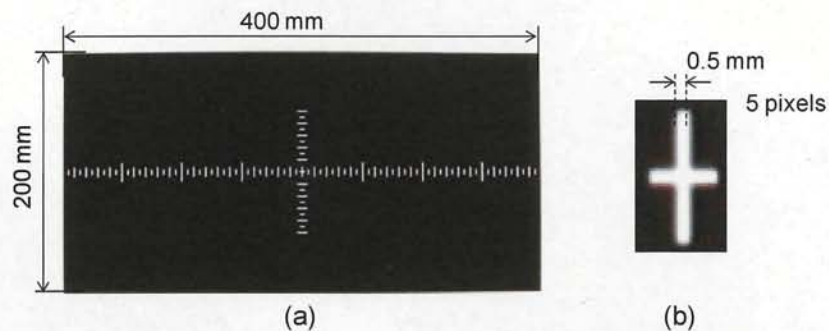


Fig. 10 Images of the template observed by the image capture system that uses a digital camera; (a) whole image and (b) magnified image.

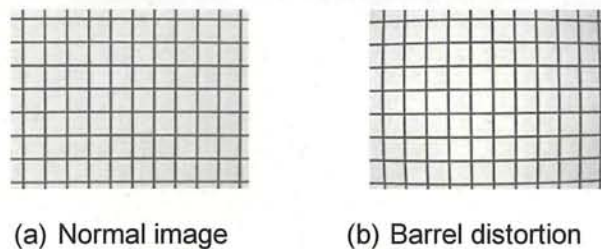


Fig. 11 Sample of the image distortion caused by a wide-angle lens; (a) normal and (b) barrel distortion.

Another problem in the digital camera system is the capturing of useless wall surfaces (Fig. 12). Figure 13 shows an example of the resulting image. Sometimes it is difficult to distinguish between the surface of the target and the wall

surface because the intensity of the wall surface image depends on the roughness of the wall surface, the in-plane location of the hole, and the tilt of the wall. Thus, this useless wall surface image affects the image processing for the edge detection.

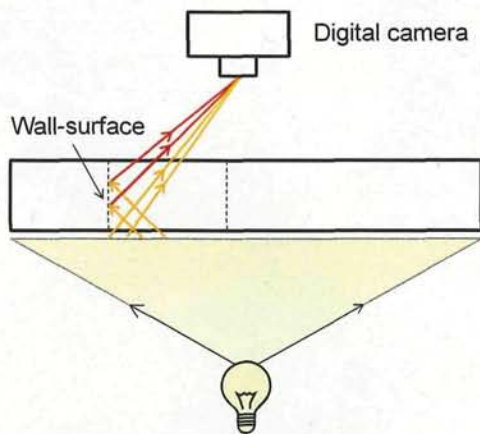


Fig. 12 Imaging of the wall surfaces.

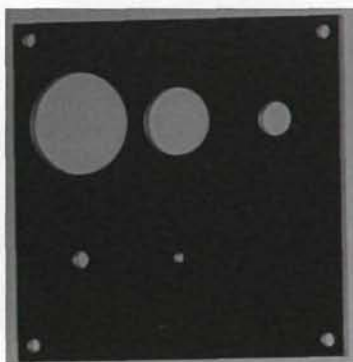


Fig. 13 Sample image captured by the digital camera.

## 4. IMAGING TECHNIQUE FOR WALL SURFACE DETECTION

### 4.1 Setup

We propose in this paper a more effective technique for optically detecting the wall surface image. It reduces burden of the image processing for the edge detection. The schematic of the setup is shown in Fig. 14. The target is slipped in between the crossed polarizers as shown in Figs. 14(a) and 14(b). Light of the correct polarization from a halogen lamp passes through the lower polarizer [1]. In Fig. 14(a), the horizontally polarized light that is transmitted by the target and the upper polarizer is detected by a digital camera. In the case of Fig. 14(b), the angle of polarization in the lower polarizer is  $45^\circ$  with respect to the horizontal line. Since no light is observed at the digital camera if the target is absent, only the images of the wall surface can be detected under the configuration shown in Fig. 14.

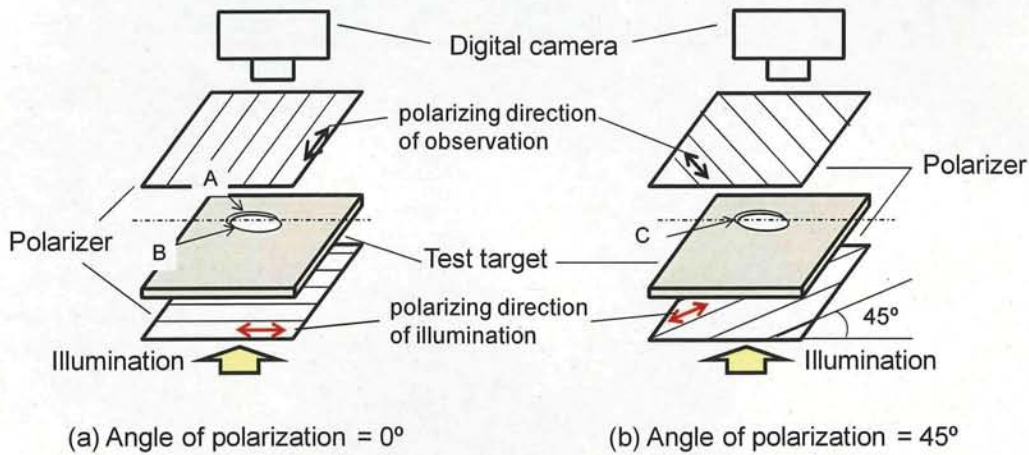


Fig. 14 Configurations for the wall surface detection.

#### 4.2 Experiment and discussion

Figure 15 explains the proposed technique. Figures 15(a) and 15(b) correspond to those of Figs. 14(a) and 14(b), respectively. The circles represent the edges of the holes, and the directions of the arrows indicate the angle of polarization of the light that passes through the lower polarizer. In the case of Fig. 14(a), the light reflected at the wall surfaces around sections A and B are depolarized because the angles between the direction of the polarization of the light and tangent at the wall surfaces become  $45^\circ$  and the lights reflect randomly at these positions [2]. In contrast, the polarization state of the light reflected at the wall surfaces around section C is almost maintained because the incident light and the tangent at the wall surface cross with an angle of  $90^\circ$  and the light reflects mostly in one direction. Since most of the depolarized light passes through the upper linear polarizer, the digital camera detects the intensity of the light and the wall surface images around sections A and B are highlighted. On the other hand, the light reflected around section C cannot pass through the upper polarizer. The image captured with the proposed setups in Fig. 14(a) is shown in Fig. 16(a). The detected wall surface image around C is dark in Fig. 16(a), while those around A and B are highlighted. Thus the bright wall surface image is observed when the crossing angle between the direction of the polarization of the light and tangent at the wall surface becomes  $45^\circ$ .

To detect the bright image around section C, the lower polarizer is rotated by  $45^\circ$  as shown in Figs. 14(b) and 15(b). In this case, since the crossing angles at sections A and B become  $0^\circ$  and  $90^\circ$ , respectively, no major depolarization occurs and no bright images are recorded by the digital camera. However, a bright image is observed around section C because the crossing angle at this position is  $45^\circ$ . We can confirm these results in Fig. 16(b).

The other configurations, where the polarization angles of the lower polarizer are  $90^\circ$  and  $135^\circ$ , respectively, are shown in Figs. 15(c) and 15(d). We confirmed that the highlighted parts in these configurations are the same as those of Figs. 15(a) and 15(b), respectively. Hence, it is sufficient to prepare only the setups shown in Figs. 15(a) and 15(b). Superposing Figs. 13, 16(a), and 16(b), we can obtain Fig. 17, in which the wall surfaces are clearly detected.

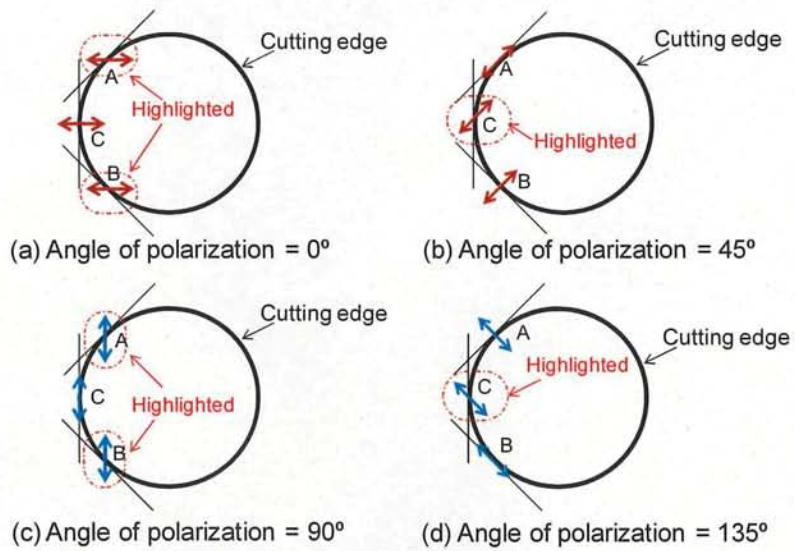


Fig. 15 Schematic of hole edges and angle of polarization.

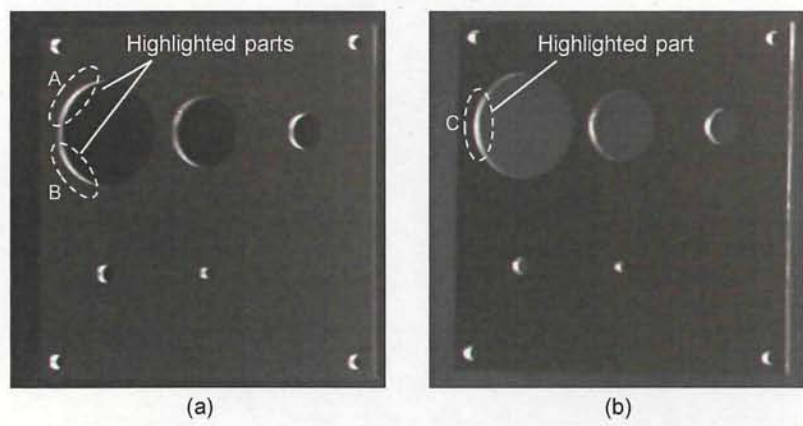


Fig. 16 Images of the wall surfaces partially enhanced with the polarizing technique.

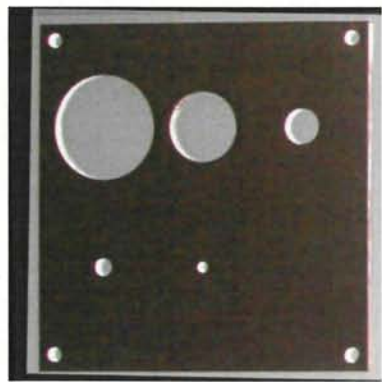


Fig. 17 Image of the wall surfaces enhanced with the polarizing technique.

## 5. SOFTWARE FOR IMAGE VERIFICATION

Finally, we explain the verification program. The flow of the process is shown in Fig. 18. The image digitized by the scanner or digital camera is filtered for noise reduction and compressed with the Bit Reduce Drawing Style Engine (called "BIRDS"), which reduces digital data by a factor of 10 to store the image data efficiently. After detecting edges and adjusting rotational direction, the data is stored in the DXF format. The DXF data obtained from the captured data is compared with the reference data in the matching stage. Also, we can measure the dimensions of the converted DXF data with the computerized caliper.

The samples of the viewing surface for the verification process are shown in Figs. 19 and 20. The converted and original DXF images are displayed on the left and right hand sides, respectively, of the Graphical User Interface (GUI), as shown in Fig. 19. We can measure the dimensions on this screen. The converted image drawn with the white lines is shown on the left hand side in Fig. 20, while the original image is shown on the right hand side. The positions of any defects that are found are highlighted with differently colored lines. The colors indicate the error range of the defects.

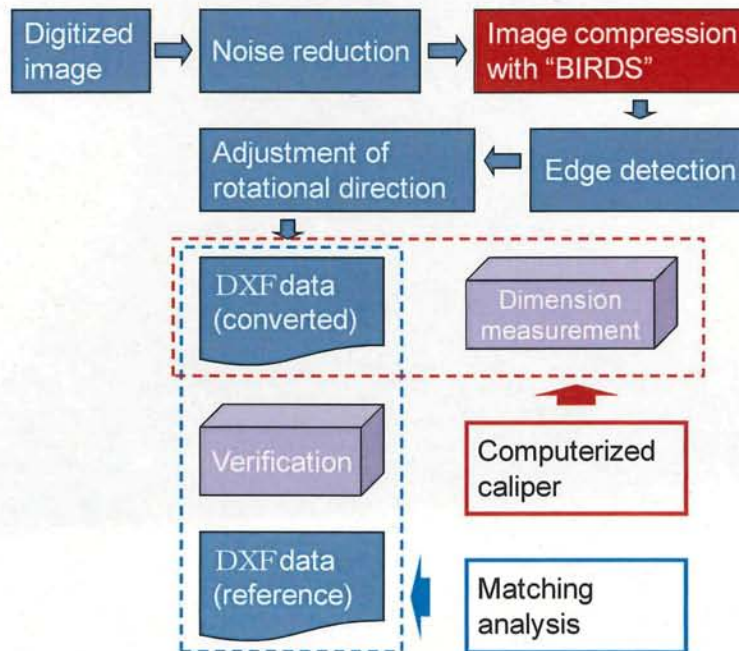


Fig. 18 Flow of the image verification process.

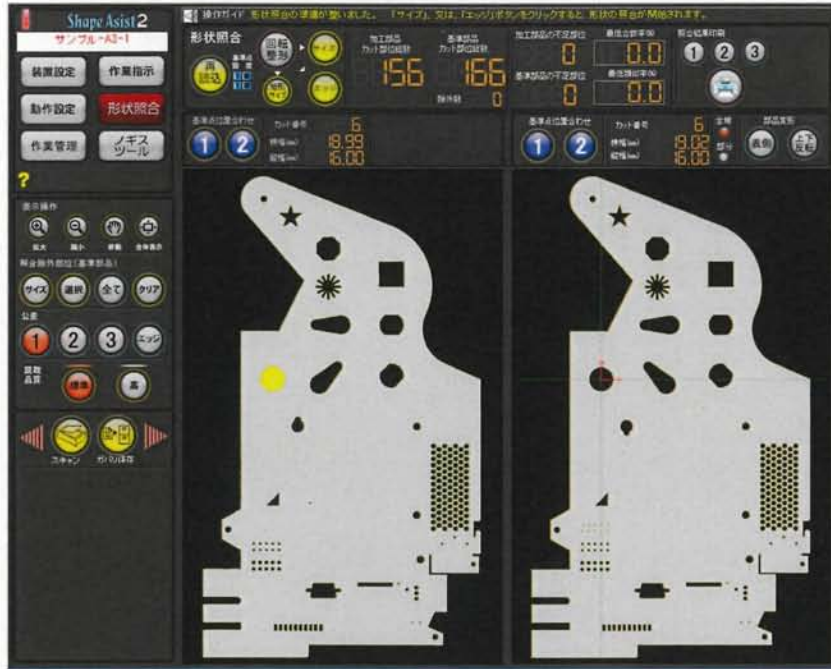


Fig. 19 Converted and original DXF images displayed in the GUI.

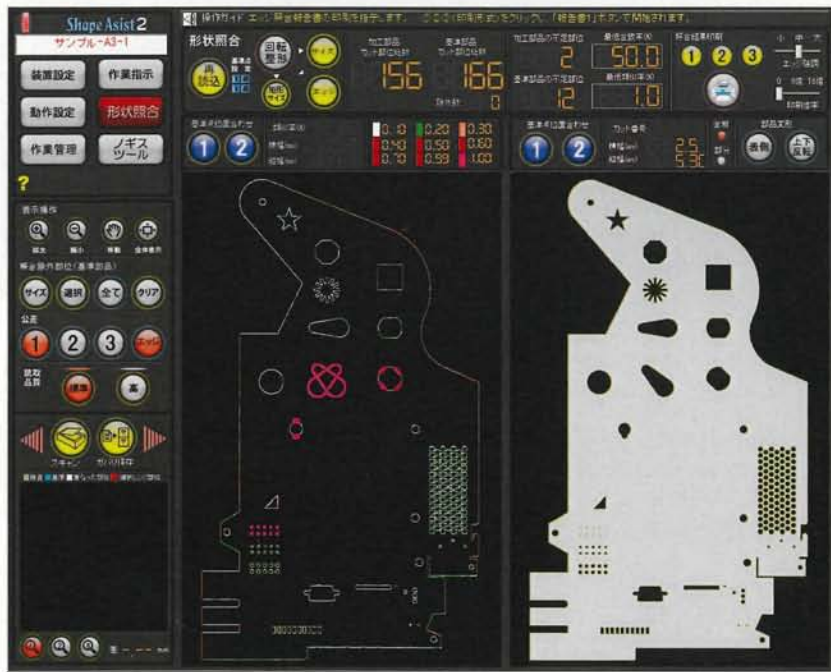


Fig. 20 Matching process between the converted edge image and original DXF image.

## **6. CONCLUSIONS**

We proposed a novel processing cycle for sheet-metal working. It uses a computerized image processing technique that automates the inspection of the products and reduces the required inspection time. The consolidated production assisted by the unified inspected data, web contents, and cross network enables an increase in the production efficiency.

## **ACKNOWLEDGEMENT**

This work was supported by the Ministry of Internal Affairs and Communications, Strategic Information and Communications R&D Promotion Programme (SCOPE) under contract 102304003.

## **REFERENCES**

- [1] E. Hecht, [Optics], Addison Wesley, Massachusetts, 326-327 (1998).
- [2] K. J. Gåsvik, [Optical Metrology], John Wiley & Sons, England, 215-227 (2002).